

BEAM LOSS SIMULATIONS FOR THE PROPOSED TATTOOS BEAMLINE AT HIPA

M. Hartmann^{*,1}, D. Kiselev, D. Reggiani, J. Snuverink, H. Zhang, M. Seidel¹
Paul Scherrer Institut, 5232 Villigen PSI, Switzerland

¹also at École Polytechnique Fédérale de Lausanne (EPFL), Lausanne, Switzerland

Abstract

IMPACT (Isotope and Muon Production with Advanced Cyclotron and Target Technologies) is a proposed initiative envisaged for the high-intensity proton accelerator facility (HIPA) at the Paul Scherrer Institute (PSI). As part of IMPACT, a radioisotope target station, TATTOOS (Targeted Alpha Tumour Therapy and Other Oncological Solutions) will allow the production of promising radionuclides for diagnosis and therapy of cancer in doses sufficient for clinical studies. The proposed TATTOOS beamline and target will be located near the UCN (Ultra Cold Neutron source) target area, branching off from the main UCN beamline. In particular, the beamline is intended to operate at a beam intensity of 100 μA (60 kW), requiring a continuous splitting of the main beam via an electrostatic splitter. Realistic beam loss simulations to verify safe operation have been performed and optimised using Beam Delivery Simulation (BDSIM), a Geant4 based tool enabling the simulation of beam transportation through magnets and particle passage through the accelerator. In this study, beam profiles, beam transmission and power deposits are generated and studied. Finally, a quantitative description of the beam halo is introduced.

INTRODUCTION

The High Intensity Proton Accelerator facility (HIPA) at the Paul Scherrer Institute (PSI) delivers a 590 MeV CW (50.6 MHz) proton beam with up to 1.4 MW beam power (2.4 mA) to spallation and meson production targets serving particle physics experiments and material research [1].

IMPACT (Isotope and Muon Production using Advanced Cyclotron and Target technologies) is a proposed upgrade project envisaged for HIPA [2]. As part of IMPACT two new target stations are foreseen to be constructed: HIMB (High Intensity Muon Beamline) focuses on increasing the rate of surface muons while TATTOOS (Targeted Alpha Tumour Therapy and Other Oncological Solutions), an online isotope separation facility, will allow to produce promising radionuclides for diagnosis and therapy of cancer in doses sufficient for clinical studies. The TATTOOS facility includes a dedicated beamline intended to operate at a beam intensity of 100 μA (60 kW beam power), requiring continuous splitting of the high-power main beam via an electrostatic splitter [4]. A realistic model of the complete TATTOOS beamline from splitter to target was established in Ref. [5] using Beam Delivery Simulation (BDSIM), a Geant4 based

program simulating the passage of particles in a particle accelerator [6].

One of the primary concerns in the operation of high-power accelerators is machine component activation caused by uncontrolled beam losses [7]. With regards to the TATTOOS beamline, the splitter in particular has to withstand significant power deposition and the beam losses due to scattering are a major challenge to be evaluated. Within this context, beam profiles and power deposits are simulated and studied. Finally, a quantitative description of the beam halo is introduced.

PROTON BEAMLINE

Overview of HIPA Facility

An overview of the HIPA facility with the foreseen TATTOOS installation is shown in Fig. 1. The proton beam is extracted from the Ring cyclotron and delivered to two meson production targets, Target M and Target E, through a dedicated beamline (PK1), along with two spallation targets for thermal/cold neutrons (SINQ) and ultracold neutrons (UCN) [1]. A fast kicker magnet diverts the full intensity beam (henceforth named main beam) from Targets M, E and SINQ to the UCN beamline via macro-pulsed kicks. Finally, the splitter located downstream of the kicker magnet in the PK1 beamline can peel off a fraction of the main beam and send it continuously to the UCN target [8]. Importantly, the fast kicker magnet and splitter cannot operate simultaneously.

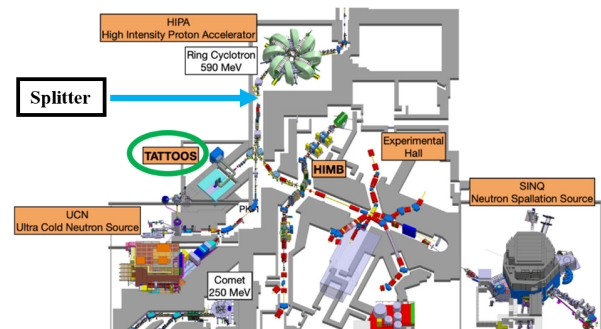


Figure 1: PSI's proton accelerator facility HIPA. The proposed TATTOOS installation is circled in green. The relative location of the splitter is also marked.

TATTOOS Beamline Description

Figure. 2 illustrates the simulated BDSIM model of the TATTOOS beamline. The beamline starts with the splitter

* marco.hartmann@psi.ch

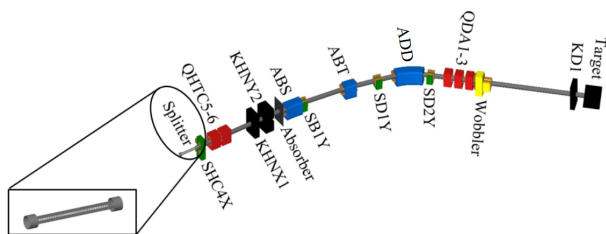


Figure 2: Complete TATTOOS beamline.

peeling off a small portion of the main beam. It consists of two cathodes (1100 mm long, 110 mm high and 30 mm thick) at a fixed voltage of -172 kV and a thin septum. The septum (1094 mm long) is located equidistant from the cathodes and consists of 175 tungsten alloy strips. Each strip is 2 mm long, 122 mm high and 0.05 mm thick. The two cathodes create two electric fields on every side of the strips that are on ground potential. The incoming protons of the main beam are thus steered away by 3 mrad from the strips at the end of the splitter for each beam. Two identical steering magnets called SHC4X on each side of the splitter compensate for the effect of the electrostatic field on the main beam and increase the deflection of the split beam. Previous simulations have demonstrated that the splitter can withstand the power deposition with approximately 20 W being deposited on the first strip.

Owing to space limitations, the first section of the UCN beamline is used for TATTOOS. Consequently, TATTOOS cannot be operated whenever a beam pulse is being delivered to UCN. In order to switch from TATTOOS to UCN operation, it is necessary to retract the splitter from the beam, while a dipole magnet (ABT) will change its polarity to bend the beam from the TATTOOS to the UCN part of the beamline. In the first section of the UCN beamline used for TATTOOS (approximately 9.5 m long) there is one quadrupole doublet, two copper collimators (KHNX1 and KHNX2) with movable jaws and a septum magnet (ABS). The combined effect of ABS and ABT will be a 13 degree bend. Further downstream, an additional dipole magnet (ADD) will bend the beam a further 32 degrees for a total of 45 degrees towards the TATTOOS beamline. Finally, a quadrupole triplet will be used to shape the beam on target. To distribute the heat on the target more uniformly, the beam will be wobbled in two dimensions. A complete description of the beamline and its components is given in Refs. [5] and [2]. Its machine protection system is described in Ref. [3].

Horizontal Split Beam Profiles

BDSIM generates a given number of protons with (x, p_x, y, p_y, t, E) from an input Gaussian beam distribution. An input file as described in Ref. [5] is used to record the phase space coordinates after the splitter (with 100 μ A peeled off from the main beam) and the horizontal profile is simulated

with one million primary protons, 0.524 m upstream of the KHNX1 collimator (Fig. 3).

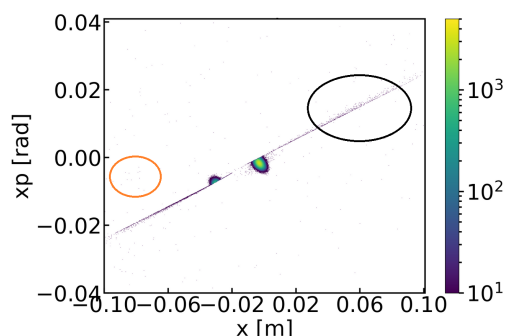


Figure 3: Horizontal phase space 0.524 m upstream of the KHNX1 collimator.

Within the context of beam loss studies, the GEANT4 toolkit in BDSIM allows to probe the full range of physics processes. In particular, the hadron-nucleus interactions of interest were characterised using the Bertini cascade model (*ffp_bert*) which is most commonly used for high energy physics applications [9, 10]. Furthermore, the physics list “*em ffp_bert decay muon hadronic_elastic em_extra*” was chosen based on the recommendations from BDSIM/GEANT4 [11].

From Fig. 3 the splitting of the main beam into two distinct bunches may be observed. In addition, various scattering processes leading to beam losses may be noticed: off-momentum protons resulting from inelastic scattering (orange circle) and a line of scattered protons due to the non-uniformity of the electric field acting on the strips (black circle).

Beamline Optics

Due to its prevalent historical application for simulating the HIPA proton channel, TRANSPORT [12, 13], was employed to design the TATTOOS beamline lattice. The TRANSPORT initial beam conditions are then fed into BDSIM. Subsequently, the beam optics from BDSIM was benchmarked with MAD-X [14] where an excellent agreement is found and reported in [5].

The beamsize of the split beam is computed along the beamline for two different split beam currents and shown in Fig. 4. In addition, the transmission of the split beam to the target is also studied and illustrated in Fig. 5. For a larger split beam current, the beam size is larger as the core of the beam is more dense with respect to the halo. As a consequence, the transmission to the target is also higher.

Finally, it is important to ensure that during TATTOOS operation, also operation up to SINQ will remain feasible. For this reason, the beam lattice from extraction of the Ring cyclotron up to the SINQ target is characterised and modelled in BDSIM. Figure. 6 illustrates the beam size in the horizontal plane along the beamline with the splitter location highlighted.

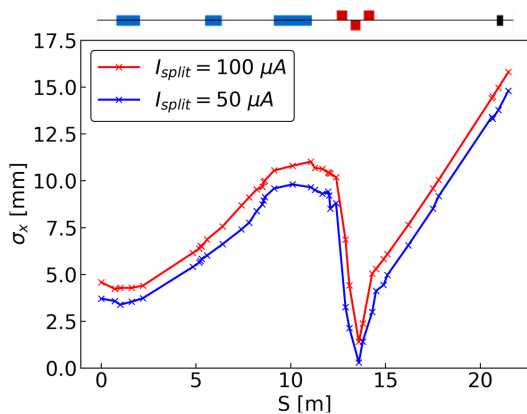


Figure 4: Horizontal beam size of split beam along the TATTOOS beamline for 100 μA (red) and 50 μA (blue) split beam currents.

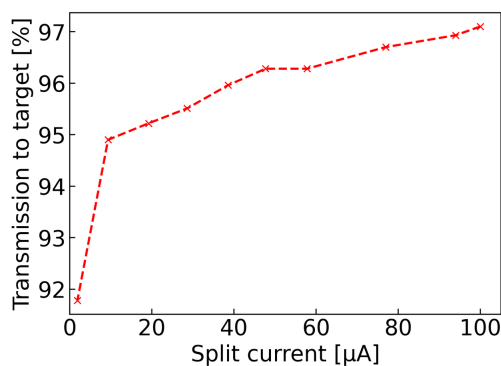


Figure 5: Transmission of split beam from splitter to TATTOOS target for different split beam currents.

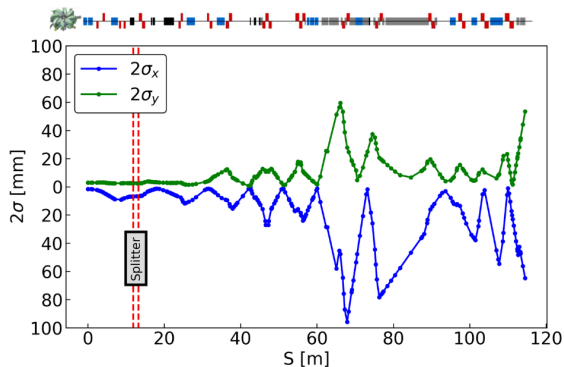


Figure 6: Beam sizes from extraction to SINQ target. Splitter location is marked with dashed red lines.

BEAM LOSS SIMULATIONS

TATTOOS and Proton Channel Losses

As mentioned previously, the monitoring and early detection of small beam losses in high energy hadron accelerators is of high importance, usually demanding to be sensitive to beam loss levels smaller than 1 W/m [15].

With high energy protons like the ones extracted from the Ring cyclotron, a very large number of secondary particles

may be produced and lost. In this regard, one aspect to be evaluated concerning the design of the TATTOOS beamline is the activation generated by head-on proton collisions of the beam with the strips of the splitter, as stated in Refs. [16] and [17]. These protons undergo angular scattering and are lost downstream along the beamline. A loss point is the end of the trajectory of a primary proton due to inelastic collisions, fragmentation or absorption in matter. In BDSIM, the energy deposition is recorded in one to three dimensional histograms made on an event-by-event basis or as a simple integration across all events.

To control the losses in the TATTOOS beamline, it was found in simulations [5] that the aperture of the two collimators KHNX1 and KHNY2 can be optimised, thereby reducing the horizontal (respectively vertical) beam halo of both main and split beams. Figure 7 shows the power deposition from splitter to target where the power deposited along the TATTOOS beamline with optimal collimator settings is compared to the case where there are no collimators.

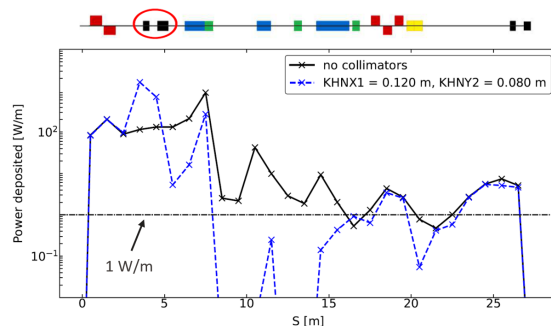


Figure 7: Power deposition from splitter to target with optimal collimator settings. Collimator positions are circled in red. 1 W/m level is marked with an arrow.

The power deposition is also studied from extraction of the Ring cyclotron to the SINQ target for the cases with and without splitter respectively (Fig. 8). An increase of the losses up to Target M is observed, as expected. This is due to the scattered particles from the splitter being lost. Further studies and measures to reduce beam losses are needed as this part of the beam line is maintained hands-on. After impacting Target M, the beam halo is cleaned [10]. As a consequence, the beam losses downstream of Target M with the splitter are comparable to the nominal case without splitter.

Beam Halo Simulations

Both experimental observations and simulations show that high-intensity beams produce halo which lead to eventual particle losses. The characteristics of the halo differ depending on the mechanism of halo production (see Ref. [18]). Recently, significant efforts have been made to attribute a general quantitative definition of the halo. One method (henceforth named distribution method), is to characterise the beam core-halo limit solely on the distribution of particles in 2D phase space. It is for example, the ratio of beam

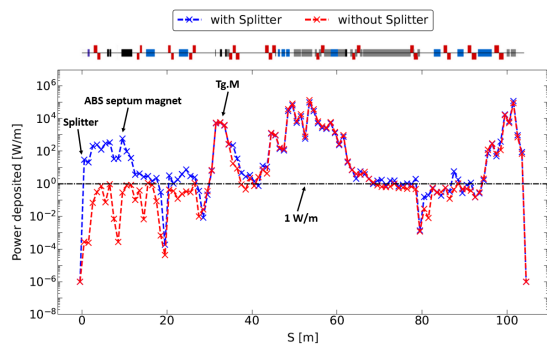


Figure 8: Power deposition from the extraction of the Ring cyclotron to SINQ target. Case with splitter in the beamline and operating at 100 μ A (blue curve) is compared to case without splitter (red curve).

sizes included in [19]:

$$\frac{m \text{ RMS}}{n \text{ RMS}} \quad (1)$$

with n being 1 and m typically 3. A Gaussian distribution is typically chosen as a reference distribution. Once the core-halo limit is established, the percentage of halo particles (PHP) may be calculated as following [19]:

$$\text{PHP} = 100 \cdot \frac{N_h}{N_c} \quad (2)$$

where, if the core-halo limit is defined by the distribution method, N_h and N_c are the number of particles contained in 3 RMS and 1 RMS of the Gaussian distribution respectively. Equation (2) has the advantage of offering a concrete quantitative characterisation of the halo at a given position and its evolution along the acceleration structure. However, for the TATTOOS beamline, the split beam distribution significantly differs from a Gaussian one with a halo tail that can be more or less pronounced compared to a Gaussian distribution. For this reason, another method (henceforth named second derivative method) based on the dynamics of the beam is used. According to Ref. [20], the definition of core-halo limit can be generalized as the location where there is the steepest density gradient variation, that is where the Laplacian of the density is maximum. In 1D, it corresponds to the second derivative's maximum. To illustrate this method, the normalised 1D horizontal profile after the ABS septum magnet is shown in Fig. 9 where the first and second derivatives of the profile are also shown. The maximum of the second derivative is approximately at $+1.5\sigma$ and -1.6σ . The method was also tested with a K-V (Kapchinsky-Vladimirsky) distribution [21] and no halo was detected, as expected.

Finally, Fig. 10 shows the evolution of the PHP in the TATTOOS beamline from 0.145 m upstream of the ABS septum magnet to the target for the two different beam halo characterisation methods (distribution and second derivative methods respectively). For both methods, significant decrease in the halo can be seen at the location of the dipole

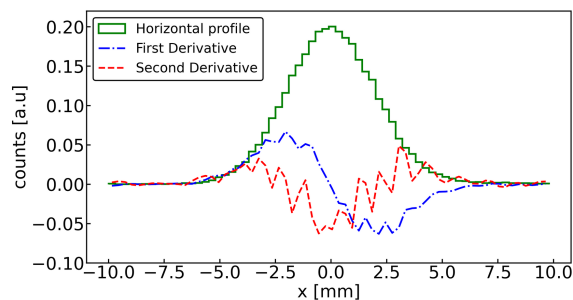


Figure 9: Normalised horizontal beam profile after the ABS septum magnet (about 8 m downstream of the splitter).

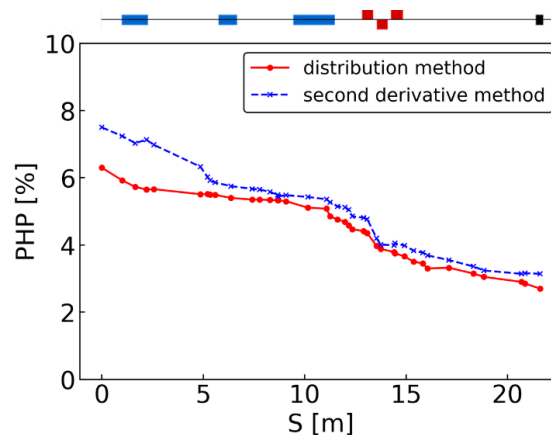


Figure 10: Evolution of the beam halo along the TATTOOS beamline for 100 μ A split beam current using two different methods.

magnets (especially at the ABS septum magnet, where main and split beam separate towards the SINQ and UCN beamlines respectively) and at the QDA2 quadrupole where the phase advance is observed to abruptly change. In general, these locations correspond quite well to the peaks in power deposition found in Fig. 7.

CONCLUSION

In this paper, realistic simulations of the TATTOOS beamline were presented using BDSIM. Several sources of beam losses were identified based on the simulated beam profiles after the splitter. In addition, power deposits both in the TATTOOS and SINQ beamlines were calculated and studied. Finally, the beam halo along the beamline was characterised using two independent methods. These simulation results will serve as model predictions for future TATTOOS beamline measurements.

REFERENCES

- [1] D. Kiselev *et al.*, “Status and future projects of the PSI High Intensity Proton Accelerator”, in *JPS. Conf. Proc.*, Tsukuba, Japan, Sep. 2019, p.01104.
doi:10.7566/jpscp.33.011004
- [2] *IMPACT Conceptual Design Report*, R. Eichler, D. Kiselev, A. Koschik, A. Knecht, N. van der Meulen, and R. Scheibl,

- Eds., Paul Scherrer Institute, Villigen, Switzerland, PSI Rep. 22-01, Jan. 2022, ISSN 1019-0643, <https://www.dora.lib4ri.ch/psi/islandora/object/psi:41209>
- [3] J. Snuverink *et al.*, “Machine protection system for the proposed TATTOOS beamline at HIPA”, presented at HB’23, Geneva, Switzerland, Oct. 2023, paper THBP04, these proceedings.
- [4] M. Olivo, U. Rohrer, and E. Steiner, “An electrostatic beam splitter for the SIN 590 MeV proton beamline”, *IEEE Trans. Nucl. Sci.*, vol. 28, pp. 3094–3096, 1981. doi:10.1109/TNS.1981.4332020
- [5] M. Hartmann *et al.*, “Design of the 590 MeV proton beamline for the proposed TATTOOS isotope production target at PSI”, in *Proc. IPAC’22*, Bangkok, Thailand, Jul. 2022, pp. 3000–3003. doi:10.18429/JACoW-IPAC2022-THPOMS023
- [6] L. J. Nevay *et al.*, “BDSIM: An accelerator tracking code with particle-matter interactions”, *Comput. Phys. Commun.*, vol. 252, p. 107200, Jul. 2020. doi:10.1109/j.cpc.2020.107200
- [7] J. Wei, “Beam cleaning in high power proton accelerators”, *AIP Conf. Proc.*, vol. 693, pp. 38–46, Dec. 2003. doi:10.1063/1.1638317
- [8] D. Reggiani *et al.*, “A macro-pulsed 1.2 MW proton beam for the PSI Ultra Cold Neutron Source”, in *Proc. PAC’09*, Vancouver, BC, Canada, May. 2009, paper TU6RFP086, pp. 1748–1750.
- [9] J. Allison *et al.*, “Recent developments in Geant4”, *Nucl. Instrum. Methods Phys. Res., Sect. A*, vol. 835, pp. 186–225, Nov. 2016. doi:10.1016/j.nima.2016.06.125
- [10] M. H. Tahar *et al.*, “Probing the losses for a high power beam”, *Nucl. Instrum. Methods Phys. Res., Sect. A*, vol. 1046, p. 167638, Jan. 2023. doi:10.1016/j.nima.2022.167638
- [11] BDSIM Manual, 2019, <http://pp.rhul.ac.uk/bdsim/manual>
- [12] K. L. Brown, F. Rothacker, D. C. Carey, and C. Iselin, “TRANSPORT - A computer program for designing charged particle beam transport systems”, CERN, Geneva, Switzerland, Rep. CERN-1980-004, Mar. 1980.
- [13] Graphic Transport/Turtle Framework, 2006, http://aea.web.psi.ch/Urs_Rohrer/MyWeb
- [14] MAD-X, 2016, <https://mad.web.cern.ch>
- [15] L. Segui *et al.*, “Micromegas for beam loss monitoring”, *J. Phys.: Conf. Ser.*, vol. 1498, p. 012045, Apr. 2020. doi:10.1088/1742-6596/1498/1/012045
- [16] E. Mariani, M. Olivo, and D. Rossetti, “An electrostatic beam splitter for the PSI 590-MeV 1-MW proton beam line”, in *Proc. EPAC’98*, Stockholm, Sweden, Jun. 1998, paper MOP27G, pp. 2129–2131.
- [17] U. Rohrer, “Modification of the EHT-splitter region”, Paul Scherrer Institute, Villigen, Switzerland, Internal Rep. 1998.
- [18] A. V. Fedotov, “Beam halo formation in high-intensity beams”, *Nucl. Instrum. Methods, Phys. Res., Sect. A*, vol. 557, pp. 216–219, Feb. 2006. doi:10.1016/j.nima.2005.10.073
- [19] P. A. P. Nghiem, N. Chauvin, W. Simeoni, and D. Uriot, “Beam halo definitions and its consequences”, in *Proc. HB’12*, Beijing, China, Sep. 2012, paper THO3A04, pp. 511–513.
- [20] P. A. P. Nghiem, M. Valette, N. Chauvin, N. Pichoff, and D. Uriot, “Core halo limit as a limit of high intensity beam internal dynamics”, in *Proc. IPAC’15*, Richmond, VA, USA, May. 2015, pp. 86–88. doi:10.18429/JACoW-IPAC2015-MOPWA006
- [21] I. M. Kapchinsky, *Theory of resonance linear accelerators*, Chur, Switzerland: Harwood Academic Publishers, 1985.